

Research Article

Designing of Elastoplastic Adaptive Truss Structures with the Use of Particle Swarm Optimization

Jacek Szklarski¹ and Marcin Wikło²

¹*Institute of Fundamental Technological Research, Polish Academy of Sciences, 02-106 Warsaw, Poland*

²*Kazimierz Pułaski University of Technology and Humanities, 26-600 Radom, Poland*

Correspondence should be addressed to Jacek Szklarski; jszklar@ippt.pan.pl

Received 13 May 2015; Accepted 11 August 2015

Academic Editor: Mohamed Ichchou

Copyright © 2015 J. Szklarski and M. Wikło. This is an open access article distributed under the Creative Commons Attribution License, which permits unrestricted use, distribution, and reproduction in any medium, provided the original work is properly cited.

In the paper we demonstrate how Particle Swarm Optimization (PSO) can be employed to solve the Adaptive Impact Absorption (AIA) problem. We consider a truss structure which is subjected to impact loads. Stiff bars can be replaced by elastoplastic fuses which control their dynamical response. The point of optimization is to maximize or minimize a given objective function by redesigning the structure. This is realized by redistributing the initial mass, finding proper fuse localizations and adjusting, in real-time, the elastoplastic limits. Comparing to the previous results, we show that PSO is capable of achieving results at least as good as gradient-based optimization, having at the same time much larger flexibility regarding the definition of the objective function. This gives significantly broader field of potential applications. In particular, we present how PSO can be used to solve the simultaneous optimization problem: mass redistribution and fuse positioning for a set of expected, various impacts.

1. Introduction

The idea of optimal structural remodeling, including topological optimization, as a problem of material distribution has been developed for decades (e.g., [1]). Consequently, there exist a large number of mathematical models and numerical tools which are capable of reliable simulation of responses of passive structures to a predefined impact scenario and improving the structure in the sense of finding an extreme of some desired objective function. The majority of practical solutions are devoted to crashworthiness analysis related to traffic collisions.

Due to the fast developing of the, so-called, smart technologies, there has been some considerable shift towards focusing on research related to adaptive structures. Various kinds of, relatively inexpensive, technical solution exist which make it possible to modify relevant structural characteristics at the moment of impact [2]. Specially designed *actuators* can be applied in real-life active structures which can adapt at required time scales (which, for obvious reasons, are small). The actuators can modify structures via various possible ways. For example, a controlled delamination process can be

applied in order to detach selected structural joints which will result in a particular response. Other possibilities include shock absorbers based on magnetorheological (MR) fluids, piezo-valves used to control pressure, and more; see, for example, [3].

Consequently, existence of appropriate technologies and mathematical solutions makes it feasible to seriously consider the potential gain from using Adaptive Impact Absorption (AIA) systems. The focus of AIA is to obtain a device which can modify its structure at the moment when a collision takes place. The point of this modification is, usually, to achieve a desired energy dissipation profile.

One of the central problems of AIA is identification of the impact and involved masses and velocities. This means that, firstly, an impact event and its location should be detected, and then the AIA system should estimate what the mass and velocity of the impacting body are. The identification should happen on timescales which enable a real-time structural modification which leads to optimal (in a given sense) absorption. This is the main difference between AIA and classical passive structural design, the ability to react to collision conditions in real-time. Impact identification is a

quite demanding, separate engineering problem on itself [4, 5] and will not be considered in this paper. Instead, we will focus on the process of optimal design of structures which can adapt by using “structural fuses.” These are elements with elastoplastic type of response with controllable yield stress. For example, in real application such fuse can be made up of MR fluid where stresses are controlled by magnetic fields. However, technical details regarding construction of these elements are not relevant in this work.

In the field of typical passive structural design, there is a huge amount of existing numerical methods and ready-to-use computer codes. However, to date, the number of existing tools for designing AIA structures is very limited. The main reason for this is that AIA is a relatively new concept, and also it differs in many aspects regarding the optimization process. Naturally, the main question which must be answered is actually the goal of optimization. This depends on the problem being solved, involved energies, if a structure should answer to a critical emergency impact or maybe periodic loads, and so forth. As a measure of success one can define minimization of accelerations, maximization of structural stiffness, somehow smoothing structural response, preserving structural integrity, or maximization of dissipated energy in some chosen time interval. Generally, the required objective function of optimization can be a very complex one.

In this paper, we consider a truss-like structure with elastoplastic fuses which can adapt to impact by adjusting the plasticity limit. The structural response is calculated by means of virtual distortion methods (VDMs) [6] and the presented results are continuation of the previous work [7, 8], where a typical gradient-based method has been used in order to achieve the desired optimization goal. The main disadvantage of gradient methods is the mathematical requirements regarding the objective function (e.g., it has to be differentiable). As mentioned, during AIA design process, one can take into account many factors: impacts with various parameters and at different geometrical places and complex goal definitions, for example, including costs of the used elements. Some problems involve solving multiobjective optimization (i.e., require simultaneous optimization of more than one objective function), which can be a particularly difficult task with any classic gradient-based approach.

All this makes it tempting to use other, possibly nonexact but otherwise versatile optimization techniques, like the ones based on the, so-called, soft computing approach, usually some sort of evolutionary computation. Using it in the structural design is a relatively new paradigm, which has a tremendous impact on the field and a vast amount of recent research is devoted to the subject. A survey can be found in, for example, [9], and a great overview regarding metaheuristic methods in structural design can be found in [10].

Here we consider the applicability of particle swarm optimization (PSO) method in the process of designing AIA structures. PSO is one of the techniques which belongs to the wide class of evolutionary computing. It is based on a set of potential solutions (called “swarm”) which is gradually improved until a certain criterion of acceptance is met. PSO is successfully applied in a very wide field of complex

engineering and scientific optimization problems, including mechanics, robotics, artificial intelligence, transportation, biology, and many more, see [11, 12]. A recent survey on PSO application in the field of electrical and electronic engineering, automation control systems, communication theory, operations research, mechanical engineering, fuel and energy, medicine, chemistry, and biology is available.

Generally, optimization of truss-like structures falls into three categories: size, shape, and topology; however even more demanding is a simultaneous optimization where the design variables describing these properties are integrated. Various techniques from the field of evolutionary computation have been applied to address these problems from the field of traditional passive design, for example, genetic algorithms [13], genetic programming [14], simulated annealing [15], or ant colony optimization [16]. However, it seems that recently one of the most popular methods is PSO, along with its various modifications.

For example, in [17], the authors applied PSO to optimize topologies of truss structures optimizing for minimum weight under stress, deflection, and kinematic stability constraints. They have considered a two-stage technique, where first topology was optimized (with modified binary PSO) and then size and shape (by means of “attractive” and “repulsive” PSO). It was reported that the methodology proposed by the authors can find superior truss structures compared with those found with classical optimization. However, simultaneous optimization for all the criteria in principle should give better results, since these design problems are not linearly separable.

Another challenging class of structural design problems are the ones which involve optimization with frequency constraints. In such problems, the search space is particularly highly nonlinear and nonconvex with numerous local optima. When using any heuristic algorithms in such cases, a need to find a balance between exploitation and exploration arises. It is of vital importance that a method explores the search space in a way which will enable it to find satisfying solution, while at the same time it will not get stuck in a local minimum. It has been shown that accordingly modified PSO algorithm was capable of dealing with such tasks [18, 19]. A recent comparison of nine metaheuristic algorithms for optimal design of truss structures with frequency constraints can be found in [20].

As in the case of frequency constraints, the classical PSO is often modified to deal with a specific problem. It is also incorporated together with other optimization techniques in order to solve problems in a more efficient way. For example, to optimize layout of truss structures, PSO has been successfully integrated with “nonclassical” methods, like cellular automata [21]. It has been demonstrated that such combination has led to better solutions and more effective convergence than in case of using “pure” PSO.

According to our knowledge, to date, there have been no results regarding usage of PSO in the AIA domain, and consequently there are no standard problems or results which we can refer to. In this work, we demonstrate how PSO can be employed in order to find optimal mass redistribution and

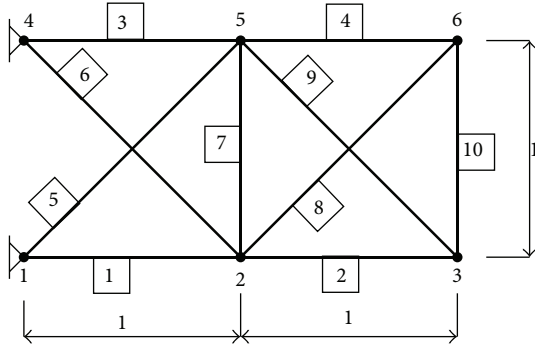


FIGURE 1: A simple truss structure, along with the used numbering scheme. Here, the horizontal/vertical distance between nodes is 1 m.

localization of structural fuses in truss structures with adaptive elastoplastic elements. Contrary to the case of passive truss structures optimization, there are no established test cases in the literature due to the innovative character of the AIA research field. In the present work, we choose to compare PSO with optimal results found by gradient methods published previously [7, 8]. It is found that, for the considered setups, PSO quickly (in ≈ 100 steps) converges to solution not worse than the ones found by means of gradient optimization. In some cases better, in the sense of the value of the objective function, structures are found.

It is shown that such PSO approach can be applied when considering multi-impact scenarios. In other words, more complex objective function is used in order to evaluate structures which are subject to a *set* of possible impacts (not just one). Moreover, it is easy to incorporate solver for optimal localization of the structural fuses (in the previous work, it has been done by replacing the stiffest elements). Since the considered optimization problem is a relatively simple one (only mass redistribution and localization of elastoplastic elements are considered) and there is a lack of previous results regarding PSO and AIA, in the current research we limit ourselves to the classical PSO, without any specific improvements.

Section 2 is devoted to short description of VDM used to evaluate the structural response, in Section 2.2 we define the optimization problem, and then in Section 2.3 we show how it can be represented as a particle swarm. Section 3 discusses the problem of mass redistribution in a truss structure in order that, with the same amount of material, minimizes/maximizes some given goal function (without any active elements). Finally, in Section 4 we show how to treat the problem if AIA elements should be incorporated in the structure.

2. The Model

As a basic model for our consideration we use a truss cantilever structure supported on one or both ends and potentially equipped with structural fuses. An example of such 10-bar structure is depicted in Figure 1. This setup has been investigated previously for various optimization goals and

constraints [22], also with PSO approach [23]. The structure is exposed to impact loads applied on one, or more, of its nodes. This means that at the moment $t = 0$ a massless node instantly increases its mass to m and its velocity from 0 to \mathbf{v} (m denoting mass of the impacting body traveling with the velocity \mathbf{v}). It is assumed that throughout calculations the node remains attached to the same bars as before the impact (there is no separation between masses and the truss). Under such circumstances, some selected quantities of interest, for example, averaged displacement, are subject to optimization. This structural model was chosen due to its simplicity (each element is associated with only one, axial, plastic distortion state) and already widely available research results regarding optimal design and active adaptation solutions. However, this does not reduce the generality of the proposed approach, which is applicable to other types of structures, for example, frame or plate structures [24].

The structural response is calculated by means of specifically designed impulse virtual distortion and impulse virtual force methods (IVDM, IVFM). VDMs are fast reanalysis methods used to compute the structural response of a modified structure in a numerically efficient way which does not require solving full set of modified structural equations. The formulation of VDM is flexible and can be easily adopted to include structural modifications like damage, plastic yielding [6], breathing cracks [25], moving masses [26], and material damping [27]. One of the advantages of VDM over other reanalysis methods, like the method of combined approximations [28], is that it requires nonparametric model of the unmodified structure (the influence matrix). With this model, calculation of responses of the modified structure can be performed faster than in other reanalysis approaches, since only one step is needed (instead of many iterations).

The details regarding VDM are beyond scope of this paper (more on this can be found, e.g., in [29]), since the focus is mainly on the process of optimization. Nevertheless, it is important to define how the adaptive elements are modeled: in Section 2.1 we briefly discuss how the structural response is calculated with elastoplastic constitutive model. Then we show how particle swarm optimization method can be applied to this optimization problem.

2.1. Modeling the Truss Structure Containing Adaptive Elements. All the details regarding the numerical simulations of the structural response of the discussed model via virtual distortion methods were presented in [7, 8] and also in [29]. Here, we limit ourselves to describing shortly the way the problem is addressed. The notation and used symbols are the same as those in the cited work: lowercase subindices i, j refer to structural elements of the truss (bars), while capital subindices M, N , and K refer to the degrees of freedom (DOF) of nodes (joints). In the two-dimensional case discussed here, there are two DOF per node, unless a node is fixed.

Generally, the equation of motion for elastic and elastoplastic structures can be stated as

$$O_{NM}\ddot{u}_M(t) + G_{Ni}^T S_{ij} [l_j(\varepsilon_j(t) - \beta_j^0(t))] = f_N(t), \quad (1)$$

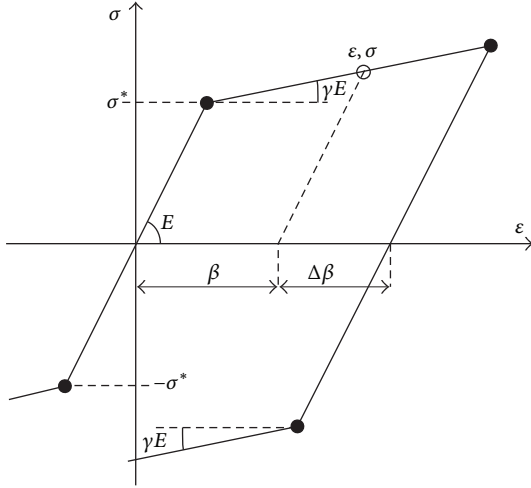


FIGURE 2: Piecewise linear elastoplastic constitutive model. Figure courtesy of Jankowski [29].

where O is the mass matrix, $u_M(t)$ denotes displacement of the M th DOF, and $f_N(t)$ is the external excitation load on the N th DOF at the time t . The total strain of the i th truss element $\varepsilon_i(t)$ obeys

$$l_i \varepsilon_i(t) = G_{iM} u_M(t). \quad (2)$$

G_{iM} is a transformation matrix, whose elements are related to the angles between elements and the directions of degrees of freedom; S_{ij} is a diagonal matrix, $S_{ii} = E_i A_i / l_i$; E_i is Young's modulus; l_i is the length of the element i ; and A_i is the cross section of the element i .

$\varepsilon_i(t)$ can be split into two parts: a purely elastic one and a plastic one, denoted by $\beta_i^0(t)$, so that

$$\sigma_i(t) = E_i (\varepsilon_i(t) - \beta_i^0(t)). \quad (3)$$

In the following only *bilinear isotropic hardening plasticity* is considered as a relatively basic example (see Figure 2) which requires for each element a single internal hardening variable $\Psi_i(t)$ called the *total plastic strain*. The evolution of $\Psi_i(t)$ in time is governed by the following simple strain hardening law:

$$\dot{\Psi}_i(t) = |\dot{\beta}_i(t)|. \quad (4)$$

The yield function $\Phi_i(\sigma_i, \Psi_i)$ is defined as

$$\Phi_i(\sigma_i, \Psi_i) = |\sigma_i| - \left(\sigma_i^* + \frac{\gamma_i E_i}{1 - \gamma_i} \Psi_i \right), \quad (5)$$

where σ_i^* , γ_i , and E_i are, respectively, the initial plastic flow stress, the hardening coefficient, and Young's modulus of the i th truss element, and the plastic modulus $\gamma_i E_i / (1 - \gamma_i)$ is determined based on a simple geometric analysis of Figure 2.

The range of admissible stresses is defined by the requirement that

$$\Phi_i(\sigma_i, \Psi_i) \leq 0. \quad (6)$$

The plastic flow ($\dot{\beta}_i^0 \neq 0$) can take place only if the stress point is on the yield surface defined by $\Phi_i = 0$. This is stated in the form of the following conditions of complementarity and persistency: $\dot{\beta}_i^0(t) \Phi_i(t) = 0$ and $\dot{\beta}_i^0(t) \dot{\Phi}_i(t) = 0$, where $\Phi_i(t) = \Phi_i(\sigma_i(t), \Psi_i(t))$. The yield function is used to define the set Y_t of indices of truss elements that are instantaneously plastic at time t :

$$(i \in Y_t) \equiv (\Phi_i(t) = 0, \dot{\Phi}_i(t) = 0). \quad (7)$$

In practice, the response of the linear structure $\varepsilon_i^L(t)$ is known in discrete time steps every Δt , and the numerical solution for the elastoplastic structure has to be advanced in the same discrete time steps. The discrete strain response of the elastoplastic structure is expressed in the following discrete form [29]:

$$\varepsilon_i(t) = \varepsilon_i^L(t) + \sum_j \sum_{\tau=0}^t D_{ij}^{\kappa\kappa}(t - \tau) \beta_j^0(\tau), \quad (8)$$

where

$$\varepsilon_i^L(t) = \sum_K \sum_{\tau=0}^t D_{iK}^{\kappa f}(t - \tau) f_K(\tau), \quad (9)$$

while $D_{iK}^{\kappa f}(t)$ and $D_{ij}^{\kappa\kappa}(t)$ are the discrete counterparts of the continuous impulse response functions. $D_{ij}^{\kappa\kappa}(t)$ is the dynamic influence matrix describing the strain evolution in the element i in the time step t , in response to a unitary impulse of virtual distortion generated in the time τ in the element j . $D_{iK}^{\kappa f}(t)$ denotes a dynamic influence matrix containing the displacement history induced in the K th DOF as a response to the unitary distortion impulse applied in the i th element.

The discrete update rules for plastic distortions of instantaneously plastic elements can be stated as

$$\Psi_i(t) = \Psi_i(t - \Delta t) + |\Delta \beta_i^0(t)|, \quad (10)$$

where $\Delta \beta_i^0(t)$ denotes the increment of the plastic strain, and

$$\Delta \beta_i^0(t) = \beta_i^0(t) - \beta_i^0(t - \Delta t). \quad (11)$$

The VDM solution is based on *trial steps*, where the plastic distortion increments $\Delta \beta_i^0(t)$ are determined in each time step t by freezing temporarily the plastic flow and performing a purely elastic step, which yields the *trial strain* $\varepsilon_i^{\text{tr}}(t)$, *trial stress* $\sigma_i^{\text{tr}}(t)$, and *trial yield function* $\Phi_i^{\text{tr}}(t)$. The trial step is performed by assuming that $\beta_i^{\text{tr}}(t) = \beta_i^0(t - \Delta t)$, $\Psi_i^{\text{tr}}(t) = \Psi_i(t - \Delta t)$. The trial strain is

$$\begin{aligned} \varepsilon_i^{\text{tr}}(t) = & \varepsilon_i^L(t) + \sum_j \sum_{\tau=0}^{t-\Delta t} D_{ij}^{\kappa\kappa}(t - \tau) \beta_j^0(\tau) \\ & + \sum_j D_{ij}^{\kappa\kappa}(0) \beta_j^0(t - \Delta t), \end{aligned} \quad (12)$$

the trial stress is

$$\begin{aligned}\sigma_i^{\text{tr}}(t) &= E_i \left(\varepsilon_i^{\text{tr}}(t) - \beta_i^{0\text{tr}}(t) \right) \\ &= E_i \left(\varepsilon_i^{\text{tr}}(t) - \beta_i^0(t - \Delta t) \right),\end{aligned}\quad (13)$$

and the corresponding trial yield function is given by

$$\begin{aligned}\Phi_i^{\text{tr}}(t) &= \Phi_i \left(\sigma_i^{\text{tr}}(t), \Psi_i^{\text{tr}}(t) \right) \\ &= \left| \sigma_i^{\text{tr}}(t) \right| - \left(\sigma_i^* + \frac{\gamma_i E_i}{1 - \gamma_i} \Psi_i(t - \Delta t) \right).\end{aligned}\quad (14)$$

The actual plastic distortions $\beta_j^0(t)$ can be found by solving

$$\begin{aligned}E_i \sum_{j \in Y_t} \left(D_{ij}^{\text{kk}}(0) - \frac{\delta_{ij}}{1 - \gamma_i} \right) \Delta \beta_j^0(t) \\ = -\Phi_i^{\text{tr}}(t) \text{sign } \sigma_i^{\text{tr}}(t).\end{aligned}\quad (15)$$

Having the above definition, the direct problem is solved time step by time step, that is, for $t = 0, \Delta t, \dots, T$. The initial conditions are assumed to be zero: $\varepsilon_i(0) = 0$, $\beta_i^0 = 0$, $\Psi_i(0) = 0$, and $Y_0 = \emptyset$. At each time step $t = \Delta t, \dots, T$, the following computations are necessary:

- (1) Trial strains, stresses, and yield functions by (12) to (14).
- (2) Temporary assumption of $Y_t = Y_{t-\Delta t}$.
- (3) Plastic distortion increments $\Delta \beta_i^0(t)$ by (15).
- (4) The corresponding strains and stresses by (3) and (8).
- (5) (a) For all the elements, verification of the yield condition defined in (6) and its compliance with the assumed set Y_t of the instantaneously plastic elements needs to be performed. (b) For elements $i \in Y_t$ verification of the stress compliance condition $\text{sign } \sigma_i(t) = \text{sign } \sigma_i^{\text{tr}}(t) = \text{sign } \Delta \beta_i^0(t)$ needs to be performed. If required, the set Y_t should be updated accordingly, and the computations should be repeated from point (3) above.
- (6) Plastic strain increments and total plastic strains by (10) and (11).

Notice that no iteration with respect to the state variables is required, which is a characteristic feature of the presented approach. Points 3–5 are repeated only if the set Y_t needs to be updated in the current time step, which happens only when an elastic element enters the plastic regime or an instantaneously plastic element is unloaded; the proper set is then usually found after just a single update.

The above assumptions are used to formulate and numerically solve a coupled problem of material redistribution (modifications of element cross sections A and associated stiffness and mass modifications). The equations are discretized in time $t = 0, 1, \dots, T$ and solved by means of Newmark scheme, T being the final time after which the construction is evaluated; that is, the value of an objective function is

calculated. For more details regarding D_{ik}^e , B_{Nk}^e , and the entire numerical procedure the reader is encouraged to refer to [7, 8] or [29].

Regarding the material properties used throughout the paper, the values are consistent with the previous work and are as follows: Young's modulus $E = 210$ GPa, the density $\rho = 7800$ kg m⁻³, and the initial cross section of all elements is 100 mm².

2.2. The Optimization Problem. Consider an initial truss structure \mathcal{S}_i consisting of the n bar elements with the same cross section $A_i = \text{const}$, $i = 1, \dots, n$, and nodes (massless) which join the bars. The structure is exposed to impact loads; that is, a mass m with given velocity \mathbf{v} is added at a node (or multiple different nodes in case of a multiple impact event). As a result, the initial conditions for \mathbf{v} and m in the node change accordingly. During the entire analysis, the mass is assumed to be attached to the node and to move together with it. In the numerical model, the mass is reflected by an appropriate modification of the mass matrix O in (1).

Let the volume of material used for \mathcal{S}_i be \bar{V} . We consider optimization problems which can be formulated as follows (divided into two classes: “design” and “adaptation”).

- (1) Design: find new element cross sections A_i' such that the corresponding material volume is equal to the initial one \bar{V} and given objective function is minimized/maximized.
- (2) Design: it is as (1) but localization of adaptive structural elastoplastic fuses is taken into account.
- (3) Adaptation: find optimal plastic limit σ^* at the moment of impact, which will minimize/maximize given objective function.

In the previous work [7, 8], optimization problems (1) and (3) were solved with the use of gradient-based method with typical pros and cons related to such approach. The gradient-based method requires a proper definition of the objective function, which has to be differentiable; it is prone to converging in a local minimum, and so forth. From the perspective of design, it is tempting to obtain complete freedom regarding definition of the objective function which can lead, for example, to handling multiple impact optimization.

2.3. The Particle Swarm Optimization. Particle swarm optimization (PSO, [11]) is a metaheuristic optimization method which iteratively tries to improve a candidate solution. As typical methods of this sort, it does not guarantee that the optimum is found; however, a very large space can be searched and there are no requirements regarding the objective function. Therefore PSO can be used for irregular, noisy, coarse problems or multiobjective optimization.

In the presented approach, the classical version of PSO is used only in the design process (cf. Section 2.2). As will be discussed later, during the impact phase, selection of the optimal plastic limit σ^* is a smooth problem with a single minimum which can be efficiently solved by gradient methods. Of course, in principle, also at this stage PSO can be used

- (1) For each particle i :
- (2) Initialize \mathbf{x} with a random value, $\mu_{\min} \leq x_j \leq \mu_{\max}$
- (3) Let the particle's best position \mathbf{p}_i will be equal to its initial one: $\mathbf{p}_i \leftarrow \mathbf{x}$
- (4) Assign to each particle its initial velocity \mathbf{v} so that each component of the vector is a random number $v_j \leftarrow (-|\mu_{\max} - \mu_{\min}|, \dots, |\mu_{\max} - \mu_{\min}|)$
- (5) Calculate the objective function for particle i $f_i(\mathbf{p}_i)$
- (6) Update the swarm best solution $\mathbf{b} \leftarrow \mathbf{x}_i$ if $f_i \leq f(\mathbf{b})$
- (7) For each particle i :
- (8) Pick random numbers r_p, r_b from the range $[0, \dots, 1]$
- (9) For each component j :
- (10) $v_{i,j} \leftarrow \omega v_{i,j} + \phi_p r_p (p_{i,j} - x_{i,j}) + \phi_b r_b (b_j - x_{i,j})$
- (11) $\mathbf{x}_i \leftarrow \mathbf{x}_i + \mathbf{v}_i$
- (12) If $f(\mathbf{x}_i) < f(\mathbf{p}_i)$ then the particle's best $\mathbf{p}_i \leftarrow \mathbf{x}_i$
- (13) Update the swarm best solution: if $f_i \leq f(\mathbf{b})$ then $\mathbf{b} \leftarrow \mathbf{x}_i$
- (14) If a given termination criterion is not met, go to (7)

ALGORITHM 1: The particle swarm optimization algorithm. For the basic AIA design problem, the particles represent consecutive elements cross sections; $x_{i,j} = \mu_j$. If, for example, the localization of structural elements is taken into account, \mathbf{x} is extended accordingly (see Section 4.1).

as an alternative (e.g., if a more complex objective function is required).

During the design phase, each candidate structure \mathcal{S} is represented as a vector of real numbers $\mathbf{x}_i = (x_{i,j=1}, x_{i,j=2}, \dots, x_{i,j=n})^T$, which is in the context of PSO entitled as a "particle." The process of relating \mathbf{x} to a structure is usually referred to as "coding" and, regarding the material redistribution, it will correspond to the ratio of modified cross section \widehat{A}_j to the original one A_j of the j th element:

$$x_j = \mu_j := \frac{\widehat{A}_j}{A_j}. \quad (16)$$

We will impose limit on the cross sections, by requiring that each component of the vector will be in range $\mu_{\min} \leq x_j \leq \mu_{\max}$, where μ_{\min} is the minimum element cross section; here $\mu_{\min} = 0$ which coincides with the element removal (which is trivial to implement, unlike in the case of gradient methods), and $\mu_{\max} = 3\mu_0$, where μ_0 is the initial cross section ratio $\mu_0 := 1$. After any modification, the particle \mathbf{x} is normalized in a way that the volume of the corresponding structure is equal to the volume of the initial one \widehat{V} , so that the amount of material needed for all the structures is identical.

With each particle \mathbf{x}_i , there is an associated vector called its velocity \mathbf{v}_i , whose elements lie in the range $[-|\mu_{\max} - \mu_{\min}|, |\mu_{\max} - \mu_{\min}|]$. Additionally, each particle i keeps track of its best position in the history of optimization \mathbf{p}_i , that is, a position for which $f(\mathbf{p}_i)$ is extreme (minimal or maximal, depending on the desired optimization objective).

Let \mathcal{N} be the set (the swarm) of N particles representing N structures. The PSO algorithm iteratively moves all the particles \mathbf{x}_i through the search space according to their velocities \mathbf{v}_i . Each particle is attracted to its all-time best position \mathbf{p}_i and to the swarm all-time best solution \mathbf{b} (updated at each step). The degree of this attractiveness, along with the particle "intention" to follow its velocity, is defined by the parameters ϕ_p , ϕ_b , and ω , respectively. The PSO algorithm for finding

optimal solution, in the sense in the sense of minimizing some utility function $f(\mathbf{x})$, is presented in Algorithm 1.

The definition of the minimized objective function $f(\mathbf{x})$ of course depends on the desired optimization goal. For example, in order to maximize structural stiffness, it can be equal to the deviation of node position from their initial location. The next section describes an example of such optimization.

One of the issues of fundamental importance when using PSO is the proper selection of the control parameters ω , ϕ_p , and ϕ_b and the population size N . Since PSO is intrinsically flexible and indeterministic, it is impossible to give a formal prescription for values of these parameters which would give the best results in a general case. Although there exists some research concerning procedures of how to adjust these values [30], possibly during the optimization process [31], often they are selected by means of a trial-and-error method. In such procedure, ω , ϕ_p , ϕ_b , and N are chosen arbitrarily in a way which reflects the nature of underlying objective function. One should keep in mind that, generally speaking, ω controls the tendency to explore the entire search space, ϕ_p the tendency to explore in the vicinity of local extrema, and ϕ_b the convergence rate to the best solution found so far. N is responsible for the diversity of potential solutions (which is also associated with the demand for computational resources).

It is clear that the PSO control parameters can be very different for various problems and it may be difficult to find satisfactory balance between exploration and convergence. In order to select values for our AIA model, we have checked how the PSO behaves for various parameter sets (≈ 30 sets) for the scenario discussed in Section 3.1. We have looked at the convergence rates and the ability to find the globally optimal solution for various, random initial conditions (keeping in mind that N should not be too large in order to constrain the computational time). This procedure led us to the following values which are used for all the calculations presented in the paper: $\omega = 0.8$, $\phi_p = \phi_b = 0.5$, and $N = 25$.

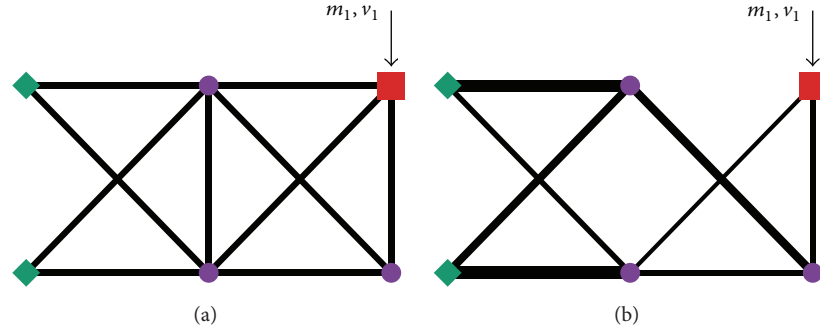


FIGURE 3: (a) Original structure: the two leftmost nodes are fixed and the node where impacting mass $m_1 = 1$ kg with the velocity $v_1 = 5$ m/s is marked with the arrow. (b) Remodeled structure which maximizes the stiffness (at the impact node at $t = 8$ ms). Here and in the subsequent figures, diamonds denote fixed points, filled circles represent the nodes, and a square marks the node where the impact takes place. The width of the lines representing elements is proportional to their cross section.

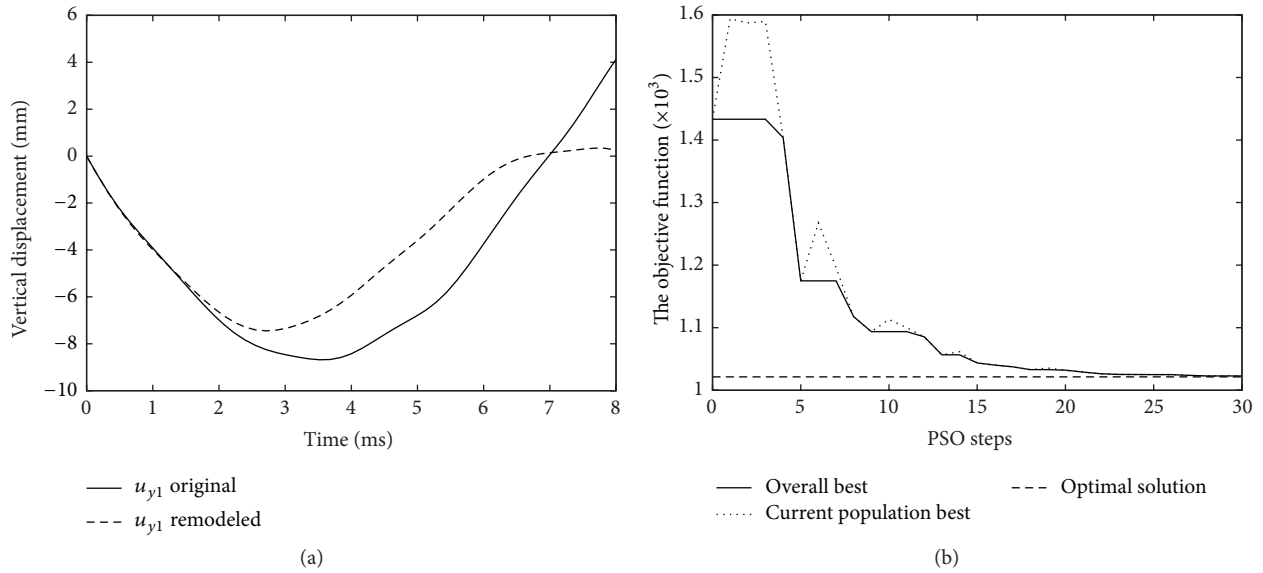


FIGURE 4: (a) Vertical deflections on the node at which the impact takes place for the original and the PSO remodeled structure. (b) Convergence of the PSO method to the optimal solution found by means of the gradient optimization (the horizontal line).

3. Remodeling without AIA Structural Fuses

3.1. Designing for a Given Impact Event. As the first example of structural PSO optimization, we consider the simple truss structure depicted in Figure 3(a), where two nodes are fixed (BCs require that the velocity is always 0) and there is one impacting mass at the node labeled with a square and an arrow. Identical setup was analyzed in [32] and direct comparison with the gradient method can be made.

As the objective function we choose

$$f(\mathbf{x}) = \sum_{t=0, \dots, T} (u_{y1} - u_{y1,t=0})^2, \quad (17)$$

where the analyzed time period is $T = 1$ ms after the impact, u_{y1} is the vertical displacement of the node at which the impact takes place, at the discrete time t , and $u_{y1,t=0} = 1$ is the node's initial position. The result of such optimization is

presented in Figure 3(b), and deflections for the original and the remodeled structures are shown in Figure 4(a).

From Figure 4(b), one can see that the PSO solution quickly converges to the best solution found by the gradient method (the horizontal line, value taken from [32]). The detailed values are presented in Table 1. In this, relatively simple, case there is one solution to which all the tried initial PSO populations have converged. This can be interpreted as the fact that it is likely that there are no local minimums in this case.

Let us consider another example: a more complex structure with two impacting masses at the same moment. Identical setup has been analyzed in [7]. The objective function will be analogous to the previous one:

$$f(\mathbf{x}) = \sum_{t=0, \dots, T} \left((u_{y1} - u_{y1,t=0})^2 + (u_{y2} - u_{y2,t=0})^2 \right), \quad (18)$$

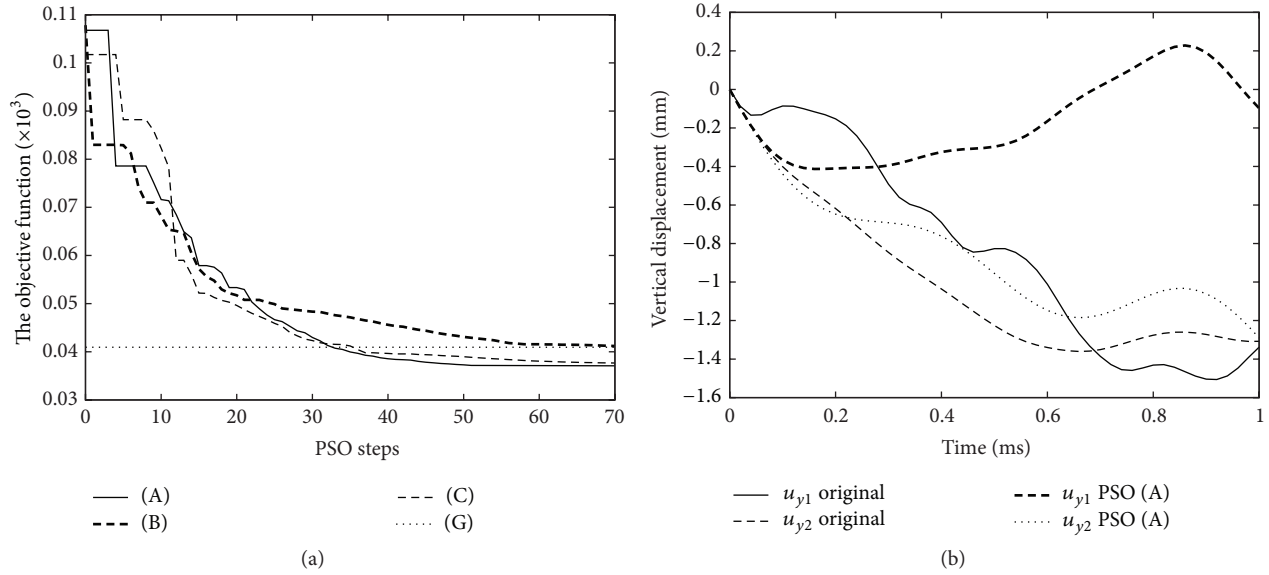


FIGURE 5: (a) Convergence of PSO for various initial populations: (A), (B), and (C); (G) represents the optimum as found by the gradient method [7]. (b) Response of the original structure and the one which is a result of PSO (A).

TABLE 1: Cross sections (mm^2) of the 10-element truss structure (Figure 1): original; optimized for maximum stiffness by the gradient method; stiffest by PSO; simultaneously optimized for maximum energy dissipation with a single adaptive element; compare Section 4.1 (* marks the optimal localization of the active element in this case).

| Elem. | Orig. | Grad. | PSO | PSO-AIA |
|-------|-------|-------|-------|---------|
| 1 | 110 | 233.3 | 233.9 | 122* |
| 2 | 110 | 103.6 | 103.1 | 0.0 |
| 3 | 110 | 205.1 | 204.4 | 70.9 |
| 4 | 110 | 0.0 | 0.0 | 306.6 |
| 5 | 110 | 142.8 | 142.2 | 45.9 |
| 6 | 110 | 95.7 | 96.8 | 189.7 |
| 7 | 110 | 0.0 | 0.0 | 0 |
| 8 | 110 | 69.1 | 69.9 | 306.6 |
| 9 | 110 | 154.3 | 153.6 | 0 |
| 10 | 110 | 87.0 | 86.5 | 0 |

where u_{y1} and u_{y2} denote the vertical location of the nodes at which the impacting masses are loaded, $T = 1$ ms.

It is understood that the exact optimization path in PSO depends on the initial swarm. Therefore various initial conditions can lead to different solutions, if there is more than one local minimum. This can be clearly seen in Figures 5 and 6, where PSO converges to distinct structures which give very similar values of the objective function. It should be noted that some of these solutions are actually *better* (i.e., give smaller value of f) than the one found by the gradient method in [7].

There is no denying the fact that the outcome of such optimization is practically unacceptable. For example, solution (B) will fail if the velocity of the left impacting mass would have, even very small, nonzero horizontal component.

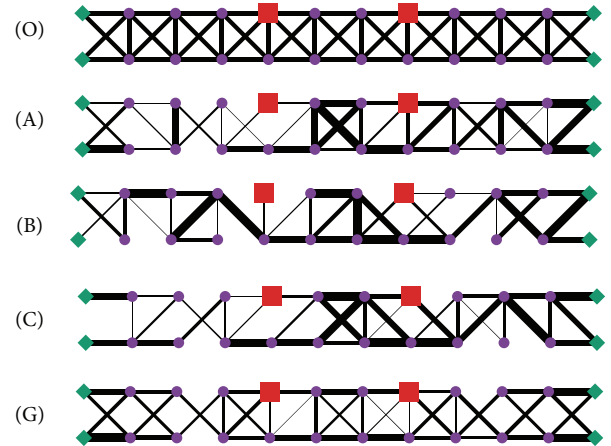


FIGURE 6: Original truss-beam structure (O) with two impacting masses, $m_1 = 0.1$ kg, $v_1 = 5$ m/s (the left node marked with a square), $m_2 = 2$ kg, $v_2 = 5$ m/s (the right one). (A), (B), and (C) denote final states of PSO for various initial conditions; (G) represents the solution obtained with the gradient optimization in [7]. Here, the total width is 1.1 m; the height is 0.1 m.

The exact final result of PSO, as any other optimization method, will strongly depend on the chosen objective function, including the integration time T . PSO starts with a swarm of completely random structures and as it happened it converged to configurations giving smaller f which is defined by (18). On the other hand, in the previous work, the starting point of the gradient method was always a structure with equal cross section for all the bars.

The example is presented here in order to show that in the entire search space of the problem, there exists better solution than the one which is found by the gradient method. This is not really surprising, bearing in mind the complexity of the

objective function and its dependence on the large number of variables. If one would like to obtain a solution which can be applied in practice, one would have, for example, exploited the potential problem symmetry or define a specific set of initial conditions for PSO (possibly, along with any kind of constraints during the optimization process). Also, performing optimization for a large set of expected impacts is desired. These issues are discussed in more detail in the following sections.

Regarding comparison of computational requirements for PSO and gradient methods, it should be noted that in the previous work the latter converged after ≈ 100 steps. For $N = 25$, this is roughly equivalent to 5 PSO steps. Looking at the convergence rates in Figures 4(b) or 5(a) one can see that there exists computational overhead when comparing to the gradient-based approach (here by the factor ≈ 5). This is usually the price one has to pay when PSO is applied. However, it is worth mentioning that PSO algorithms are trivial to parallelize, and it is easy to implement them on widely available multiprocessor platforms.

3.2. Designing for Multiple Impact Events. One of the limitations of the gradient-based optimization in the discussed structural design process is the difficulty of definition of a differentiable objective function which would evaluate a structure for multiple various impacts. This can be easily achieved with PSO. Consider a scenario in which a structure can be potentially loaded with an impact characterized by 4-tuples, n , m , v , and p , where n is the node number at which the impacting mass m with the velocity v is applied; the probability of such event is p . Let \mathcal{I} be the set of all N_I expected impacts (i.e., such 4-tuples); $\sum_{i=0, \dots, N_I} p_i = 1$. Then the objective function which takes into account the possibility of multiple impacts can be defined as

$$f'(\mathbf{x}) = \sum_{i=0, \dots, N_I} \frac{p_i}{N_I} \left(\frac{f(\mathbf{x} | \{n_i, m_i, v_i\})}{f(\mathbf{x}_o | \{n_i, m_i, v_i\})} \right)^k, \quad (19)$$

where $f(\mathbf{x} | \{n_i, m_i, v_i\})$ denotes the calculated objective function for the structure corresponding to the particle \mathbf{x} , provided that the impact is at the node n_i with given mass m_i and velocity v_i . \mathbf{x}_o is the optimal structure designed for the impact $\{n_i, m_i, v_i\}$ and k controls the penalty for deviation from $f(\mathbf{x}_o)$ (we use $k = 2$).

The normalization with respect to \mathbf{x}_o requires precalculation of the optimal value for a single impact. This assures that the input from any impact to the total objective function f' is proportional only to the probability p_i (and not, e.g., to the impacting mass, where smaller mass would lead to much smaller deflections). This procedure is particularly important when expected impacts significantly differ in kinetic energy.

As an example, let us consider the structure presented in Figure 7, where an impact is expected at any node in the upper part, except the ones which are fixed. The impacting mass/velocity pairs are drawn from the set $\{2 \text{ kg}, 5 \text{ m/s}\}$, $\{0.5 \text{ kg}, 10 \text{ m/s}\}$. All the events are assumed to be equiprobable. The objective function for each single impact $f(\mathbf{x} | \{n_i, m_i, v_i\})$ is the same as that in (17); that is, the deflections

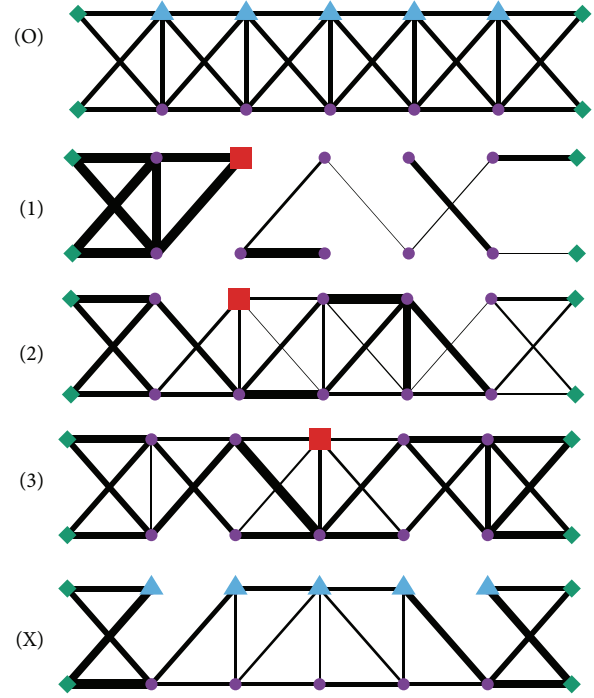


FIGURE 7: (O) Original structure which is a subject to multiple possible loads. (1)–(3) A sample optimum PSO remodeling for a single impact at the marked nodes, $m = 2 \text{ kg}$, $v = 5 \text{ m/s}$ (1), and $m = 0.5 \text{ kg}$, $v = 10 \text{ m/s}$ (2, 3). (X) A PSO remodeled structure optimized for multiple impact classes, \mathbf{x}'_o . The triangles in (X) represent places of potential impacts.

at the impacting node are minimized. For example, (1) is optimized for a single impact with $m = 2 \text{ kg}$, $v = 5 \text{ m/s}$, at the node marked with a square. Note that, according to the limits on cross section stated in Section 2.3, the bars on the leftmost side could not exceed $\mu_{\max} = 3\mu_0$. During the optimization process, these elements reached μ_{\max} . The remaining elements have virtually no influence on f for this impact and, consequently, the remaining mass is randomly distributed among these bars.

In case of the multiple impact optimization, using f' , PSO converged to a final solution depicted in Figure 7(X), and the final value of $f'(\mathbf{x}'_o) = 4.032$. This should be interpreted as that the final structure performs, on average, two times worse (for $k = 2$) than the one optimized for a given impact. Ideally, f' would be equal to unity, which would mean that the structure is perfectly optimized for all the possible impacts (of course, usually it is impossible).

4. Adaptation to Impact Loads

Up to this moment, we have discussed the process of redesigning structures in order to maximize stiffness. As mentioned in Introduction, an essential part of any AIA system is responsiveness at the moment of an impact. In our scenario this can be realized when some elements act as structural fuses, that is, have properly adjusted plastic limit; see (3). It is reasonable to assume that the dissipated plastic-like energy

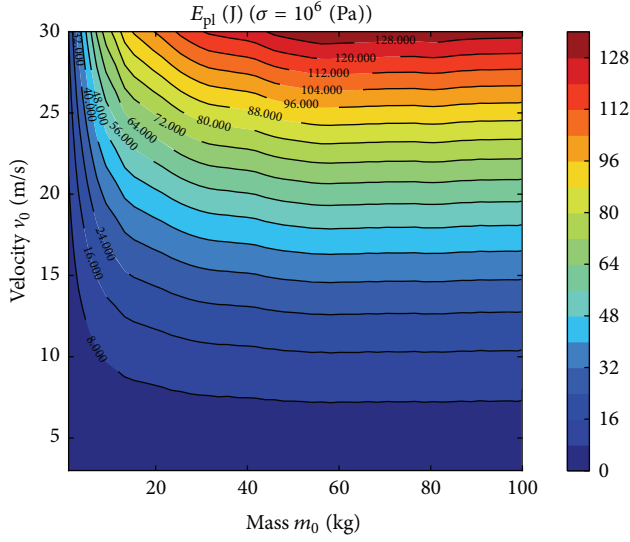


FIGURE 8: Absorbed plastic energy (in J) as a function of the impacting mass and velocity for a truss structure as in Figure 3, where element number 1 has $\sigma = \text{const} = 10^6$.

E_{pl} in some given time $T = 1$ ms should be maximized (as in [8]):

$$E_{\text{pl}} = \sum_{t=1, \dots, T} \sum_{i=1, \dots, N_A} \sigma_i(t) \Delta \beta_i^0(t) l_i A_i, \quad (20)$$

where $i = 1, \dots, N_A$ denotes the active elements.

As a basic example consider the structure from Figure 3(a), where element number 1, connecting nodes 1 and 2, is replaced by an elastoplastic one. Setting the elastoplastic limit to the constant value $\sigma^* = 10^6$ Pa leads to energy absorption which depends on the impacting mass and its velocity. Such dependence is plotted in Figure 8.

Assuming that a structural geometry is given, along with the location of the active elements, the AIA problem at the moment of impact is twofold: identification of the impacting mass and velocity and finding the plasticity limits σ^* for all the active elements. As stated in Introduction, impact identification with simultaneous mass and velocity identification is a difficult task on itself and is beyond the scope of this paper. For given m and v , the dependence of optimal σ^* can be calculated for the truss structure with 10 elements (Figure 3); it is depicted in Figure 9.

Naturally, using active elements with real-time σ^* adjustment will give some benefit only if the dissipated energy is significantly larger than in case of some constant σ^* chosen during the design process. The potential gain is shown in Figure 9(b) where one can clearly see that, in the given range of impacting masses, active response can dissipate 7-8 times more energy than the passive elastoplastic construction. Remarkably, for the considered structure and location of the active element, the optimal plasticity limit depends mostly on the impacting mass and not the velocity.

Using PSO at the moment of impact in order to adjust σ^* is, in principle, possible; however it would be somehow extravagant, at least if the objective function like the one

defined in (20) is considered. Having information about the impacting m and v , a gradient-based real-time method can be applied without any problems. Another practical solution would be to calculate the optimal plastic limits offline and then use them in a tabulated form during a real impact.

In this AIA problem, PSO can bring on two other major improvements. Firstly, in the previous work, the location of structural fuses was rather guessed than selected on some formal basis. The reason for such procedure was due to problems with the proper definition of objective function which would take position of the active elements into account. PSO can be deployed to find optimal location of active elements for a given structure. However, the second potential gain is the possibility of solving a problem of *simultaneous* material redistribution and structural fuses location. In the next subsection we will look at an example of the latter.

4.1. Using PSO for Simultaneous Material Redistribution and Structural Fuses Location.

Let us again consider the truss structure from Figure 3. This time, the goal will be to maximize the dissipated energy E_{pl} by using AIA fuse which should be located in place of one of the elastic elements. From the PSO point of view, this will be realized by modifying representation of the structure as a particle \mathbf{x} . Let the new, extended representation \mathbf{x}' be $\mathbf{x}' = (\mathbf{x} \ \mathbf{y})$, where \mathbf{y} is yet another vector with the length equal to number of the elements (i.e., equal to the length of \mathbf{x}). The range of possible values as the elements of \mathbf{y} is $\langle 0, \dots, 1 \rangle$ (instead of μ_{\min} and μ_{\max} as in the algorithm description, Section 2.3). Now, let the active AIA element be located at the position corresponding to the maximal y_i (or the one with the smallest i , if there exists more than one maximal y_i). If more than one of the active elements is expected, one can localize them in i_1, i_2, \dots places, so that $y_{i_1} \leq y_{i_2} \leq \dots \leq y_{i_{i_1} \neq i_2 \neq \dots}$.

The extended particle representation \mathbf{x}' is used to calculate the objective function for the structure with the material distribution defined by \mathbf{x} and the AIA elements location by \mathbf{y} . Note that this, quite versatile, way of coding can be used in order to achieve any desired goals of the structural optimization during the design process. Of course, the cost of AIA element (and consequently their total number in any structure) can be straightforwardly incorporated. PSO provides a surprisingly efficient mechanism for finding optimal solution of problems defined in a complex and noncontinuous way.

Assume that one of the elements of the 10-element examples from Figure 3 ((a)/(b) i.e., original/stiff) is replaced by a single adaptive element. By means of a brute-force method, we can trivially check how much plastic-like energy is dissipated for the given impact parameters ($m_1 = 1$ kg, $v_1 = 5$ m/s, i.e., with energy 25 J) for all the possible locations of the adaptive element. It turns out that the structure remodeled for maximum stiffness can give only slightly better results. In the case of original structure, maximum $E_{\text{pl}} = 7.14$ J is observed when the adaptive element is at the link number 1. For the remodeled structure, maximum $E_{\text{pl}} = 8.42$ J is obtained when the link number 8 is adaptive; see Table 2.

Using PSO makes it possible to simultaneously search for optimal cross section of the elements and the localization of

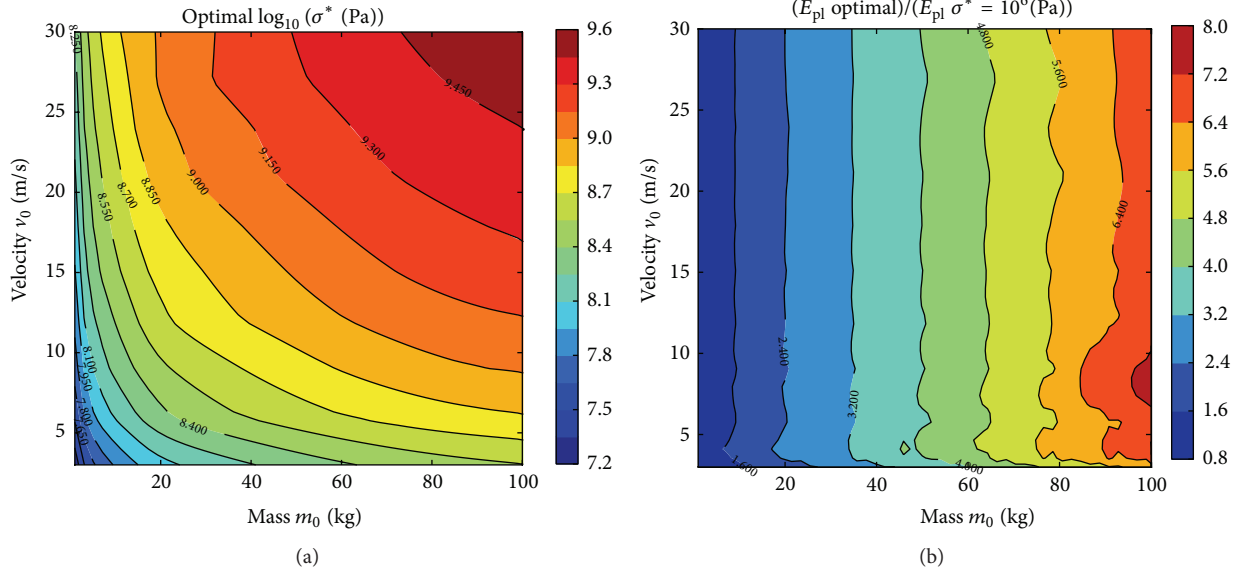


FIGURE 9: (a) The optimal elastoplastic limit σ^* leading to the largest plastic-like energy dissipation (20), as a function of the impacting mass and velocity. (b) The potential gain in using the optimal σ^* over the constant one $\sigma^* = 10^6$ Pa.

TABLE 2: Plastic-like energy E_{pl} (in J) dissipation for optimal stress yield σ^* (in MPa) for various locations of the adaptive element (instead of the elastic one) for different 10-element trusses: original (Figure 3(a)), remodeled for maximal stiffness (Figure 3(b)), and optimized by PSO (Figure 10(A)). $E_{pl}(t)$ is shown in Figure 11 for the cases marked with boldface.

| El. | Original | | Stiff | | PSO | |
|-----|------------|----------|------------|-------------|------------|--------------|
| | σ^* | E_{pl} | σ^* | E_{pl} | σ^* | E_{pl} |
| 1 | 133 | 7.14 | 49 | 7.17 | 133 | 14.10 |
| 2 | 37 | 3.85 | 65 | 6.14 | — | — |
| 3 | 133 | 7.10 | 75 | 5.87 | 178 | 10.20 |
| 4 | 75 | 5.17 | 931 | 0.05 | 34 | 10.82 |
| 5 | 60 | 2.82 | 70 | 4.97 | 21 | 0.57 |
| 6 | 100 | 2.58 | 178 | 7.81 | 75 | 9.45 |
| 7 | 1 | 0.82 | — | — | — | — |
| 8 | 87 | 2.16 | 191 | 8.42 | 32 | 13.49 |
| 9 | 37 | 2.25 | 100 | 3.76 | — | — |
| 10 | 12 | 2.38 | 70 | 4.76 | — | — |

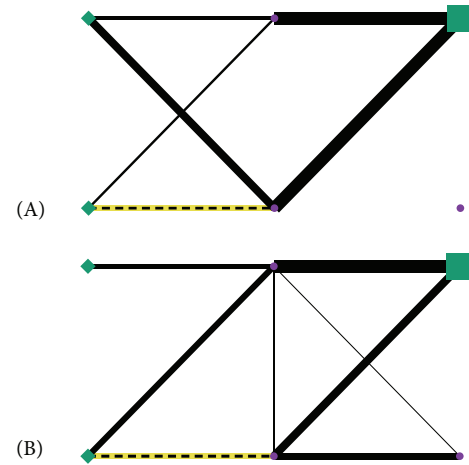


FIGURE 10: Structure from Figure 3 remodeled for maximal energy dissipation $E_{pl} = 14.10$ J. The location of the active element, as found by PSO, is marked with the dashed line. (B) An alternative solution giving slightly smaller dissipation $E_{pl} = 13.7$ J, however, with a different absorption characteristic; compare Figure 11.

the adaptive dissipators. Figure 10 depicts a sample outcome of such optimization, and one can see that the structure differs significantly from the one optimized for stiffness only. The gain regarding the dissipated energy is significant in this case, maximal $E_{pl} = 14$ J.

We should note that, in the previous work, the location of adaptive elements was chosen rather on reasonable presumptions than on optimization outcome. Moreover, this was done on structures optimized, in the first stage, for maximum stiffness. In order to address this problem with gradient optimization, one can simply consider brute-force calculations for all possible locations of active elements. However, in case of complex structures with many structural fuses, this

approach will quickly become computationally intractable, while still the issue of *simultaneous* mass redistribution and fuses localization is not taken into account.

As stated above, initially the swarm consists of completely random particles (i.e., structures), and it is possible that for larger structures PSO will evolve towards a “bizarre” result, for example, Figure 6. Such outcome formally gives near-optimal value of the objective function; however, the common sense indicates that such solution is rather impractical. Figure 12 depicts two results of PSO optimization for maximal plastic-like energy absorption for the 29-element

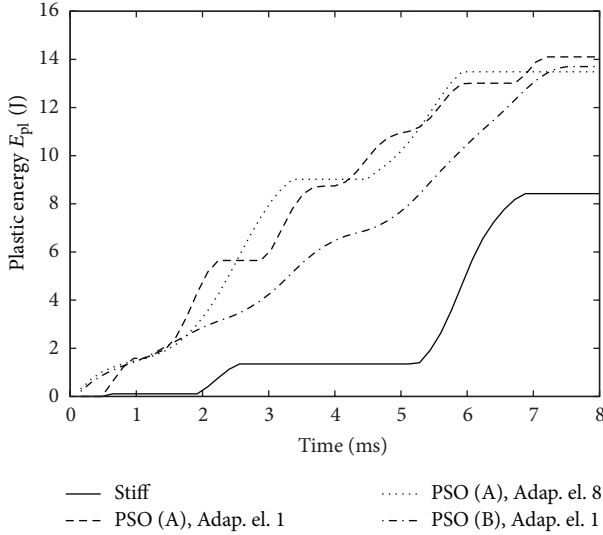


FIGURE 11: Absorption of plastic-like energy after an impact at $t = 0$ for various structures and localization of the adaptive element; compare Figure 10 and Table 2.

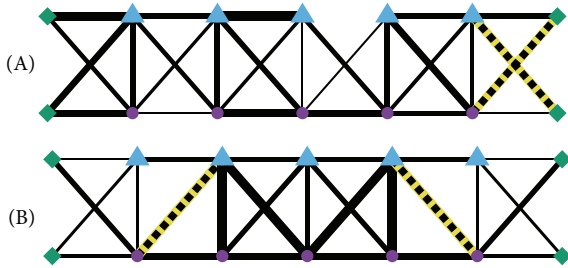


FIGURE 12: Schematic representation of the outcome of PSO optimization for the structure as in Figure 7 with two adaptive elements. (A) An example of a nonsymmetric “bizarre” result giving $E_{pl} = 19.9$ J. (B) Result under the assumption of symmetry which is taken into account in the particle coding procedure, $\bar{E}_{pl} = 25.4$ J.

structure supported on both sides, as in Figure 7. Simultaneous optimization for mass redistribution and localization of two adaptive elements (with the same σ^* , for simplicity) for the set of 10 possible impacts was performed ($\{2 \text{ kg}, 5 \text{ m/s}\}$ or $\{0.5 \text{ kg}, 10 \text{ m/s}\}$ at each of the 5 nodes marked with a square). In other words, the objective function is to maximize

$$\bar{E}_{pl} = \frac{1}{10} \sum_{n_i=1, \dots, 10} E_{pl} | n_i, \quad (21)$$

where n_i numbers the possible impacts and $E_{pl} | n_i$ is calculated for the impact n_i , 1 ms after the event, σ^* being optimally adjusted at the impact moment for maximizing the energy absorption.

The structure depicted in Figure 12(A) is characterized by the objective function $\bar{E}_{pl} = 19.9$ J. One expects that for the problem defined in the way described above the outcome should be a symmetric structure since all the nodes have equal probability of being loaded with the same conditions. Nevertheless, PSO evolved from random initial condition

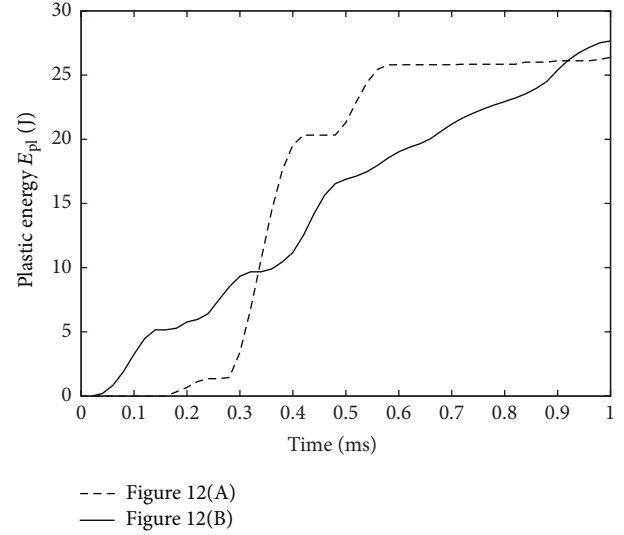


FIGURE 13: Absorption of energy E_{pl} by the two structures depicted in Figure 12. The impact takes place at the leftmost node marked with a triangle, $m = 0.5 \text{ kg}$, $v = 10 \text{ m/s}$.

to this clearly nonsymmetrical configuration with two fuses located next to each other.

Generally, larger problems require searching a huge parameter space and it is not surprising that the swarm gets stuck in a local minimum which clearly is not a suitable solution. In PSO it is easy to incorporate particle coding which exploits symmetry and any other features expected regarding the outcome of optimization. The benefit is twofold: the result more suited to expectations and reduced search space. An example of PSO result with a coding which retains structural symmetry is shown in Figure 12(B), in this case $\bar{E}_{pl} = 25.4$ J. This is a superior value to that for case (A); moreover, the symmetric solution has better absorption characteristics in the sense that is closer to a linear one; see Figure 13.

Finally, note that the structure presented in Figure 7(X) evolved from random swarm towards a symmetric configuration (although not perfectly symmetric) which reflects the boundary conditions. In principle, by appropriate modification of the swarm size and PSO control parameters, similar results can be achieved for more complex structures with fuses. For even more demanding, multimodal problems, a specific modification of PSO should be employed, for example, [33].

5. Conclusions and Outlook

We have used one of the versatile, metaheuristic optimization techniques, the particle swarm optimization, in the numerical process of designing structures which are able to actively adapt to impacts. AIA systems form a relatively new branch of mathematical problems in engineering with many subtopics open to research. Up to now, the considered AIA truss structures have been optimized only by classical gradient-based approaches. One of the drawbacks of such methods is the need of “mathematically proper” definition

of continuous objective functions. This makes it difficult to design structures which can, for example, adapt to a set of possible impacts.

We have shown that in the context of AIA design, PSO can

- (i) efficiently reproduce results previously obtained by means of the gradient optimization (Section 3.1),
- (ii) easily provide *alternative solutions* with similar values of the objective function (Section 3.1),
- (iii) be used to find out optimal structures where the *objective function is constructed from multiple various impact responses* and therefore obtain results which are optimized for *a given set of expected impacts* (Section 3.2),
- (iv) be used to search the space for *location of the structural fuses* (unlike the gradient methods); this can be even done *simultaneously* with mass redistribution and the outcome of such optimization can be *completely different* compared with the previous results obtained with gradient methods (Section 4.1).

As mentioned in Section 1, generally such structural optimization should simultaneously solve for size, shape, and topology. Incorporating AIA adds here yet another variable, namely, solving for location of the structural fuses. Following the presented preliminary research, the future work will be focused on simultaneous optimization which will include also topology, not only adaptive element localization and mass redistribution. Additionally, more complex impact scenarios will be considered; for example, various angles of the velocity vector of the impacting mass will be taken into account.

Conflict of Interests

The authors declare that there is no conflict of interests regarding the publication of this paper.

Acknowledgment

This project was financed from the funds of the National Science Centre (Poland) allocated on the basis of decision no. DEC-2012/05/B/ST8/02971.

References

- [1] M. P. Bendsoe and N. Kikuchi, "Generating optimal topologies in structural design using a homogenization method," *Computer Methods in Applied Mechanics and Engineering*, vol. 71, no. 2, pp. 197–224, 1988.
- [2] J. Holnicki-Szulc and L. Knap, "Adaptive crashworthiness concept," *International Journal of Impact Engineering*, vol. 30, no. 6, pp. 639–663, 2004.
- [3] J. Holnicki-Szulc, Ed., *Smart Technologies for Safety Engineering*, John Wiley & Sons, 2008.
- [4] K. Sekuła, C. Graczykowski, and J. Holnicki-Szulc, "On-line impact load identification," *Shock and Vibration*, vol. 20, no. 1, pp. 123–141, 2013.
- [5] Ł. Jankowski, "Off-line identification of dynamic loads," *Structural and Multidisciplinary Optimization*, vol. 37, no. 6, pp. 609–623, 2009.
- [6] P. Kołakowski, M. Wikło, and J. Holnicki-Szulc, "The virtual distortion method—a versatile reanalysis tool for structures and systems," *Structural and Multidisciplinary Optimization*, vol. 36, no. 3, pp. 217–234, 2008.
- [7] M. Wikło and J. Holnicki-Szulc, "Optimal design of adaptive structures: part I. Remodeling for impact reception," *Structural and Multidisciplinary Optimization*, vol. 37, no. 3, pp. 305–318, 2009.
- [8] M. Wikło and J. Holnicki-Szulc, "Optimal design of adaptive structures part II. Adaptation to impact loads," *Structural and Multidisciplinary Optimization*, vol. 37, no. 4, pp. 351–366, 2009.
- [9] R. Kicinger, T. Arciszewski, and K. De Jong, "Evolutionary computation and structural design: a survey of the state-of-the-art," *Computers and Structures*, vol. 83, no. 23-24, pp. 1943–1978, 2005.
- [10] A. H. Gandomi, X.-S. Yang, S. Talatahari, and A. H. Alavi, *Metaheuristic Applications in Structures and Infrastructures*, Elsevier, Newnes, Australia, 2013.
- [11] M. Clerc, *Particle Swarm Optimization*, ISTE, Wiley, 2010.
- [12] X. Hu, Y. Shi, and R. C. Eberhart, "Recent advances in particle swarm," in *Proceedings of the IEEE Congress on Evolutionary Computation*, vol. 1, p. 90, Portland, Ore, USA, June 2004.
- [13] K. Deb and S. Gulati, "Design of truss-structures for minimum weight using genetic algorithms," *Finite Elements in Analysis and Design*, vol. 37, no. 5, pp. 447–465, 2001.
- [14] Y. Yang and C. Kiong Soh, "Automated optimum design of structures using genetic programming," *Computers & Structures*, vol. 80, no. 18-19, pp. 1537–1546, 2002.
- [15] O. Hasançebi and F. Erbatır, "Layout optimisation of trusses using simulated annealing," *Advances in Engineering Software*, vol. 33, no. 7–10, pp. 681–696, 2002.
- [16] G.-C. Luh and C.-Y. Lin, "Optimal design of truss structures using ant algorithm," *Structural and Multidisciplinary Optimization*, vol. 36, no. 4, pp. 365–379, 2008.
- [17] G.-C. Luh and C.-Y. Lin, "Optimal design of truss-structures using particle swarm optimization," *Computers & Structures*, vol. 89, no. 23-24, pp. 2221–2232, 2011.
- [18] H. M. Gomes, "Truss optimization with dynamic constraints using a particle swarm algorithm," *Expert Systems with Applications*, vol. 38, no. 1, pp. 957–968, 2011.
- [19] A. Kaveh and A. Zolghadr, "Democratic PSO for truss layout and size optimization with frequency constraints," *Computers & Structures*, vol. 130, pp. 10–21, 2014.
- [20] A. Kaveh and A. Zolghadr, "Comparison of nine meta-heuristic algorithms for optimal design of truss structures with frequency constraints," *Advances in Engineering Software*, vol. 76, pp. 9–30, 2014.
- [21] S. Gholizadeh, "Layout optimization of truss structures by hybridizing cellular automata and particle swarm optimization," *Computers & Structures*, vol. 125, pp. 86–99, 2013.
- [22] U. T. Ringertz, "On methods for discrete structural optimization," *Engineering Optimization*, vol. 13, no. 1, pp. 47–64, 1988.
- [23] L. J. Li, Z. B. Huang, and F. Liu, "A heuristic particle swarm optimization method for truss structures with discrete variables," *Computers & Structures*, vol. 87, no. 7-8, pp. 435–443, 2009.
- [24] J. Holnicki-Szulc and J. T. Gierlinski, *Structural Analysis, Design and Control by the Virtual Distortion Method*, Wiley, Chichester, UK, 1995.

- [25] Q. Zhang, Ł. Jankowski, and Z.-D. Duan, "Identification of coexistent load and damage," *Structural and Multidisciplinary Optimization*, vol. 41, no. 2, pp. 243–253, 2010.
- [26] Q. Zhang, Ł. Jankowski, and Z.-D. Duan, "Simultaneous identification of moving masses and structural damage," *Structural and Multidisciplinary Optimization*, vol. 42, no. 6, pp. 907–922, 2010.
- [27] M. Mroz, Ł. Jankowski, and J. Holnicki-Szulc, "VDM-based identification of localized, damage induced damping," in *Proceedings of the 5th European Workshop on Structural Health Monitoring*, pp. 988–993, July 2010.
- [28] U. Kirsch, "Reanalysis and sensitivity reanalysis by combined approximations," *Structural and Multidisciplinary Optimization*, vol. 40, no. 1–6, pp. 1–15, 2010.
- [29] Ł. Jankowski, *Dynamic Load Identification for Structural Health Monitoring*, vol. 2 of *IPPT Reports*, Institute of Fundamental Technological Research, Polish Academy of Sciences, 2013.
- [30] Y. Shi and R. C. Eberhart, "Parameter selection in particle swarm optimization," in *Evolutionary Programming VII*, V. W. Porto, N. Saravanan, D. Waagen, and A. E. Eiben, Eds., vol. 1447 of *Lecture Notes in Computer Science*, p. 591, Springer, Berlin, Germany, 1998.
- [31] J. Wang, "Particle swarm optimization with adaptive parameter control and opposition," *Journal of Computational Information Systems*, vol. 7, no. 12, pp. 4463–4470, 2011.
- [32] M. Lo, *Projektowanie urządzeń adaptacyjnych poddawanych obciążeniom udarowym [Ph.D. thesis]*, IPPT PAN, Warszawa, Poland, 2007.
- [33] G. Zhang and Y. Li, "Parallel and cooperative particle swarm optimizer for multimodal problems," *Mathematical Problems in Engineering*, vol. 2015, Article ID 743671, 10 pages, 2015.



Hindawi

Submit your manuscripts at
<http://www.hindawi.com>

